

1 **Bayesian Deep Learning framework for Uncertainty-Aware Intrusion Detection**
2 **to enhance the Security in High Dense WSN**
3

4 VENKATESWARI .P* and SHANMUGASUNDARAM .N*, AVS College of Technology, india
5

6 Wireless Sensor Networks (WSNs) are vulnerable to evolving cyber threats, necessitating robust intrusion detection systems (IDS) that
7 quantify uncertainty to enhance decision-making. This research presents a Bayesian Deep Learning (BDL) framework for uncertainty-
8 aware intrusion detection in WSNs, leveraging probabilistic neural networks to model uncertainty in predictions. Traditional deep
9 learning IDS lack uncertainty estimation, leading to overconfident but erroneous classifications. The proposed approach combines
10 the Monte Carlo Dropout algorithm and Bayesian Neural Networks (BNNs) to provide probabilistic outputs, enabling the system to
11 distinguish between certain and uncertain predictions. The proposed framework integrates temporal feature extraction with Bayesian
12 inference for robust anomaly detection. The model achieved 99.5% accuracy, 97.5% precision, 96.5% recall, 98.5% f1-score, 95.5%
13 detection rate and 4.1% false alarm rate. The results demonstrate that uncertainty-awareness is critical for trustworthy IDS in dynamic,
14 resource-constrained WSN environments.
15

16
17 Additional Key Words and Phrases: Sensors, Networks, Bayesian Deep Learning, Uncertainty, Intrusion Detection, Wireless, Anomaly
18 Detection
19

20 **ACM Reference Format:**

21 Venkateswari .P and Shanmugasundaram .N. 2018. Bayesian Deep Learning framework for Uncertainty-Aware Intrusion Detection to
22 enhance the Security in High Dense WSN. In *Proceedings of Make sure to enter the correct conference title from your rights confirmation*
23 *email (Conference acronym 'XX)*. ACM, New York, NY, USA, 25 pages. <https://doi.org/XXXXXXX.XXXXXXX>
24

25 **1 Introduction**
26

27 Uncertainty-aware intrusion detection refers to systems that account for uncertainties in data, network dynamics,
28 and attack patterns to improve detection accuracy. WSNs are prone to uncertainties due to unreliable communication,
29 sensor noise, and evolving threats [1]. Traditional intrusion detection systems may generate false alarms or miss
30 attacks if they ignore these uncertainties. Uncertainty-aware IDS is essential because WSNs operate in unpredictable
31 conditions where data loss, noise, and dynamic topology changes are common [2]. Conventional IDS often fail to adapt,
32 leading to high false-positive or false-negative rates [3]. The attackers exploit these uncertainties to evade detection. For
33 instance, low-power jamming or spoofing attacks may mimic natural network fluctuations [4]. An uncertainty-aware
34 approach improves robustness by quantifying doubt in observations, enabling adaptive responses to both known and
35 emerging threats, thus ensuring better security in critical applications like military surveillance or environmental
36 monitoring [5]. Several challenges arise in uncertainty-aware intrusion detection. Data unreliability due to packet loss
37 or sensor errors complicates threat analysis [6]. Resource constraints (limited energy, computation, and memory) restrict
38
39

40 *Both authors contributed equally to this research.
41

42 Authors' Contact Information: Venkateswari .P, pvenkateswari@mymail.yahoo.com; Shanmugasundaram .N, nshanmugasundaram@mymail.yahoo.com, AVS
43 College of Technology, Salem, Tamil Nadu, India.
44

45 Permission to make digital or hard copies of all or part of this work for personal or classroom use is granted without fee provided that copies are not
46 made or distributed for profit or commercial advantage and that copies bear this notice and the full citation on the first page. Copyrights for components
47 of this work owned by others than the author(s) must be honored. Abstracting with credit is permitted. To copy otherwise, or republish, to post on
48 servers or to redistribute to lists, requires prior specific permission and/or a fee. Request permissions from permissions@acm.org.
49

50 © 2018 Copyright held by the owner/author(s). Publication rights licensed to ACM.
51

52 Manuscript submitted to ACM
53

54 Manuscript submitted to ACM
55

complex detection algorithms [7]. Dynamic attack patterns (e.g., zero-day exploits) demand adaptive models. The high false alarms from environmental noise reduce system trust. The scalability issues arise in large-scale deployments where centralized detection becomes impractical [8]. These factors collectively degrade detection efficiency and increase vulnerability. Hybrid approaches combining lightweight machine learning (e.g., Bayesian networks, federated learning) with probabilistic reasoning can enhance accuracy while conserving resources to mitigate these challenges [9]. Redundant data validation and trust-based neighbor collaboration reduce false alarms. Adaptive algorithms can dynamically update detection rules against evolving attacks [10]. Decentralized or hierarchical IDS architectures improve scalability, distributing computational loads. The energy-efficient cryptographic techniques and anomaly detection thresholds tuned to network conditions can further optimize performance, ensuring reliable intrusion detection despite uncertainties [11]. Traditional machine learning (ML) and deep learning (DL) models struggle to effectively capture uncertainty in intrusion detection due to several inherent limitations [12]. Most ML/DL models are designed to provide deterministic predictions rather than probabilistic confidence estimates, making it difficult to distinguish between true attacks and uncertain or noisy observations [13]. Supervised learning approaches rely heavily on labeled datasets, which often lack comprehensive coverage of all possible attack variations and environmental uncertainties, leading to overconfidence in incorrect predictions. Many models do not incorporate explicit uncertainty quantification mechanisms, which are crucial for assessing confidence levels in dynamic and noisy WSN environments [14]. Deep learning models, while powerful, are particularly prone to overfitting in small or imbalanced datasets, further amplifying uncertainty misestimation. The black-box nature of complex DL architectures makes it challenging to interpret and calibrate uncertainty, resulting in unreliable intrusion alerts under real-world conditions where data ambiguity is common [15]. These limitations highlight the need for more robust uncertainty-aware techniques to improve intrusion detection reliability. The key contributions of proposed research work have the following. • The proposed research combines deep neural networks with Bayesian probability to quantify uncertainty in intrusion detection, improving reliability in noisy WSN environments. It provides probabilistic confidence scores for predictions, distinguishing between certain and uncertain detections to reduce false positives/negatives. • The proposed model optimizes computational efficiency using variational inference or Monte Carlo dropout, ensuring feasibility in resource-constrained, large-scale deployments. It handles incomplete, noisy, and adversarial data by leveraging Bayesian inference, making the system resilient to sensor errors and dynamic attack patterns. • The proposed model provides interpretable uncertainty metrics (e.g., entropy, prediction intervals) to aid security analysts in decision-making. It reduces computational overhead through lightweight Bayesian approximations, extending the WSN node lifetime while maintaining security. Remaining parts of the manuscript has organized as the following. Section-2 illustrates the detailed explanation about the materials and methods. Section-3 demonstrates the results and Section-4 explained the complete details about the performance analysis. Section-5 provides the conclusion and future scope of proposed research work.

2 Materials and Methods

High-density WSNs face unique security challenges due to their large-scale deployments, resource constraints, and dynamic environments. Traditional IDS often struggle with false positives and false negatives and adaptability in such settings. Uncertainty-aware intrusion Detection addresses these issues by incorporating probabilistic reasoning, confidence estimation, and adaptive decision-making, making it crucial for securing dense WSNs. Table 1 shows the comprehensive analysis of existing models.

Table 1. Comprehensive Analysis

Author	Year	Model	Advantage	Limitation
Karthikeyan, M., et al. [16]	2024	Firefly Algorithm + ML	Optimized feature selection	High computational overhead
Liu, G., et al. [17]	2022	Improved kNN	Low complexity, real-time detection	Sensitive to imbalanced data
Pan, J. S., et al. [18]	2021	Lightweight ML-based IDS	Low resource usage	Less robust against advanced attacks
Ramana, K., et al. [19]	2022	WOCRU-IDS (Whale + GRU)	High accuracy	Complex, not ideal for low-power WSNs
Sadia, H., et al. [20]	2024	ML-based IDS	Detects multiple attack types	Needs large labeled datasets
Alsahli, M. S., et al. [21]	2021	SVM and RF	Helps choose best network level	Less precision and sensitive to imbalanced data
Jingjing, Z., et al. [22]	2022	MC-GRU	Captures temporal dependencies well	High memory usage
Arkan, A., et al. [23]	2023	Unsupervised hierarchical IDS	No need for labeled data	Higher false positives
Talukder, M. A., et al. [24]	2024	ML + SMOTE-Tomek	Handles imbalanced data well	Increased computational cost
Saleh, H. M., et al. [25]	2024	SGD-based IDS	Fast convergence	May get stuck in local optima
Ahmed, O., et al. [26]	2024	Context-aware ML	Better detection with context	Increased complexity
Subramani, S., et al. [27]	2023	Multi-Objective PSO	Effective feature selection	Premature convergence in PSO
Safaldin, M., et al. [28]	2021	Binary GWO + SVM	High accuracy	SVM scalability issues
Jin, J., et al. [29]	2021	Unspecified ML model	Realistic simulation	Lack of model details
Madhuri, K., et al. [30]	2022	Node-level IDS	Specialized for drop attacks	Limited to specific attacks
Otair, M., et al. [31]	2022	Hybrid GWO-PSO	Better optimization	High computational complexity
Hussain, K., et al. [32]	2022	WOA-ABC + CNN	High accuracy with deep learning	Needs large data/resources

2.1 Research Gap Analysis

- Existing uncertainty-aware IDS struggle with real-time processing in ultra-dense networks. Lightweight, distributed detection mechanisms need to be incorporated to handle massive data flows efficiently.
- Most IDS rely on static uncertainty models, failing to adapt to dynamic WSN conditions. Incorporate adaptive Bayesian or fuzzy logic-based uncertainty modeling for node mobility and link fluctuations.
- Uncertainty modeling increases computational overhead, reducing node lifetime. Energy-aware sensing techniques should be incorporated to balance accuracy and power consumption.
- Current IDS use either probabilistic or non-probabilistic methods. For improved detection, hybrid uncertainty fusion combining multiple approaches needs to be incorporated.

2.2 Research Novelty

- The proposed framework provides predictive uncertainty to assess intrusion detection confidence. It enables WSNs to distinguish between uncertain predictions (due to noise) and true attacks, reducing false positives.

- Bayesian Neural Networks treat weights as probability distributions rather than fixed values, making them resilient to adversarial evasion attacks. The proposed model has Monte Carlo Dropout (MC-Dropout) at inference time. It allows sampling-based uncertainty estimation without retraining.
- The proposed framework can learn from limited labeled data using Bayesian active learning. Here, Uncertainty-guided sampling selects the most informative data points for labeling, improving efficiency.
- The proposed dynamically adjusts detection thresholds based on uncertainty levels and reduces false negatives in high-noise WSN environments.
- The proposed framework can be optimized for resource-constrained WSNs using Bayesian approximation techniques. It enables low-latency uncertainty-aware detection at the edge.

2.3 System Design

The proposed Uncertainty-Aware Intrusion Detection System (UA-IDS) for high-density WSNs follows a modular, adaptive architecture designed to enhance security while accounting for uncertainty. Fig.1 shows the construction of the proposed design

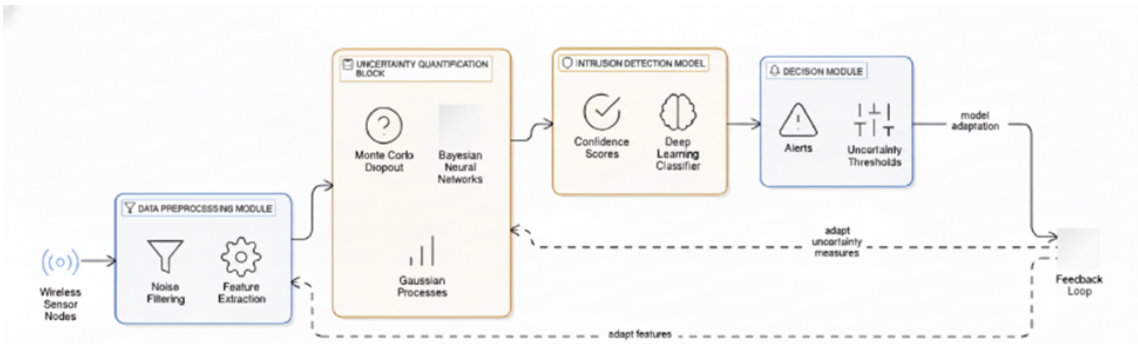


Fig. 1. This is a figure. Schemes follow the same formatting

WSN sensor nodes collect raw data, which is preprocessed by a data processing module that performs noise filtering (e.g., Kalman filtering) and feature extraction (e.g., statistical, temporal features). The uncertainty quantification block leverages Monte Carlo Dropout (MC-Dropout), Bayesian Neural Networks (BNNs), and Gaussian Processes (GPs) to estimate both aleatoric (data noise) and epistemic (model uncertainty). These uncertainty measures feed into an intrusion detection model, which combines deep learning classifiers with confidence scores to distinguish true attacks from false alarms. The decision module applies dynamic uncertainty thresholds to trigger alerts—high-confidence detections generate immediate warnings, while uncertain predictions undergo further analysis. The system incorporates a feedback loop where anomalies and uncertainty trends are detected, and the model is refined to ensure adaptability. The model adaptation mechanism adjusts uncertainty measures (e.g., recalibrating dropout rates) and feature selection (e.g., discarding noisy features) based on real-time performance. This closed-loop design enables continuous improvement, making the UA-IDS robust against evolving threats and dynamic WSN conditions.

```

209
210
211
212
213
214
215
216
217
218
219
220
221
222
223
224
225
226
227
228
229
230
231
232
233
234
235
236
237
238
239
240
241
242
243
244
245
246
247
248
249
250
251
252
253
254
255
256
257
258
259
260

```

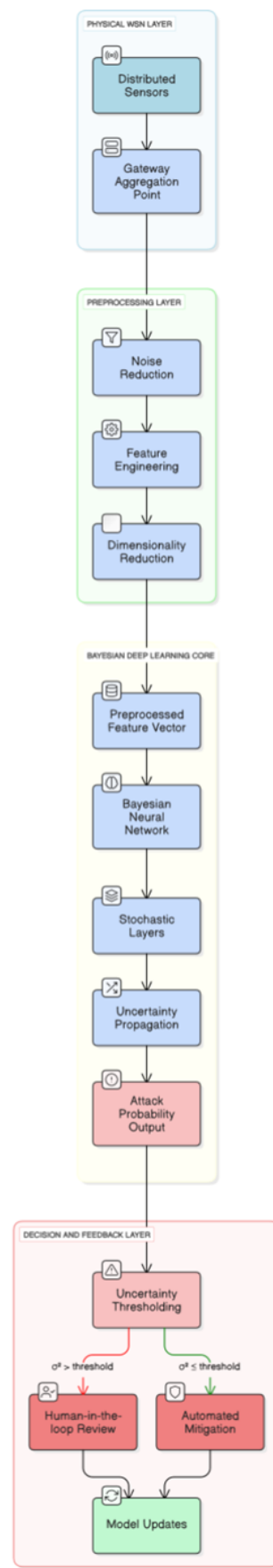


Fig. 2. Bayesian Neural Network Architecture

261
262
263
264
265
266
267
268
269
270
271
272
273
274
275
276
277
278
279
280
281
282
283
284
285
286
287
288
289
290
291
292
293
294
295
296
297
298
299
300
301
302
303
304
305
306
307
308
309
310
311
312

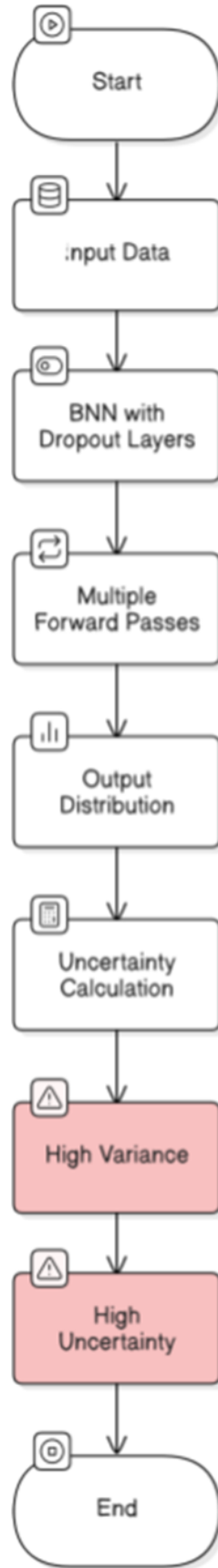


Fig. 3. Monte Carlo Dropout Sampling Process

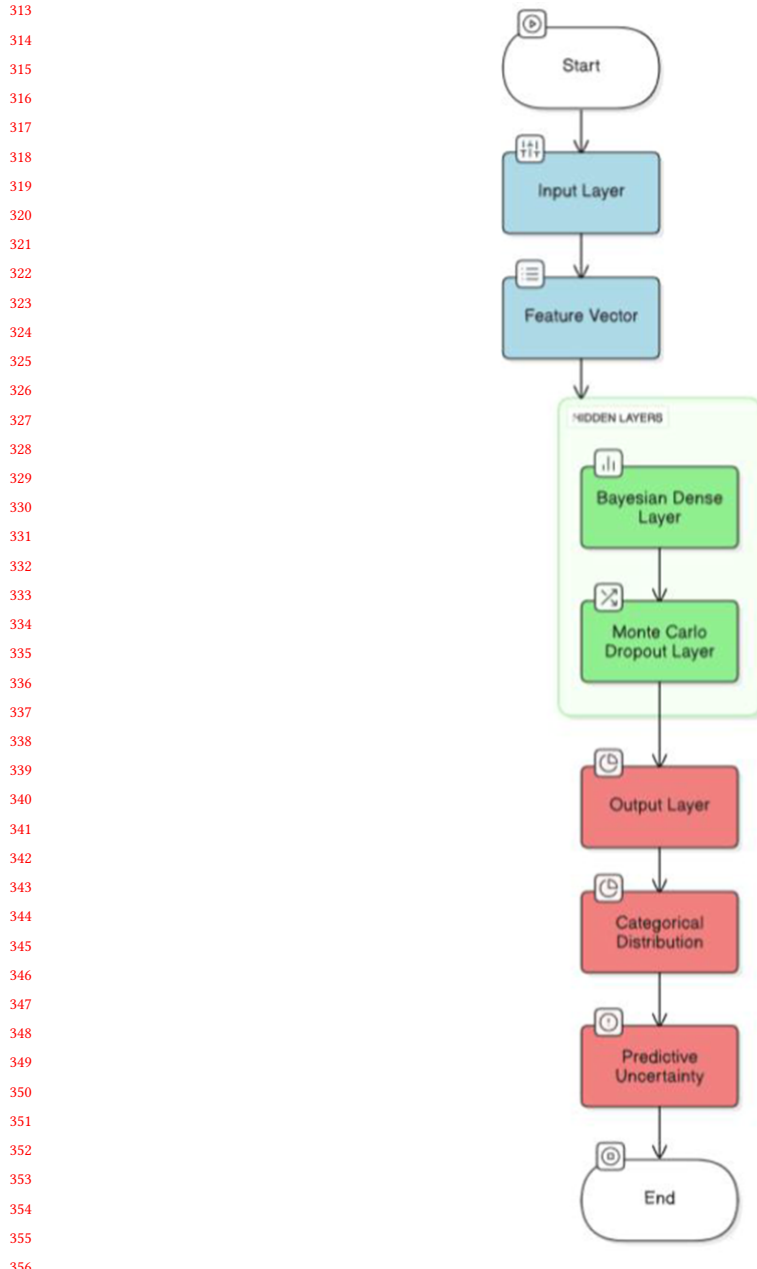


Fig. 4. Uncertainty-Aware Decision Workflow

365 2.4 Bayesian Neural Network Architecture

366 The proposed framework operates across four key layers to enhance security in high-density Wireless Sensor Networks
 367 (WSNs):

- 369 • **Physical WSN Layer :** This layer comprises distributed sensor nodes and collects raw network traffic and
 370 environmental data. Adversarial exposure are highlighted, and data is aggregated at a central gateway node for
 371 further processing.
- 373 • **Preprocessing Layer :** Raw sensor data undergoes noise reduction to mitigate environmental interference.
 374 Feature engineering extracts discriminative attributes, followed by dimensionality reduction to optimize com-
 375 putational efficiency for resource-constrained nodes.
- 377 • **Bayesian Deep Learning Core :** The pre-processed feature vector $\mathbf{X} \in \mathbb{R}^d$ is fed into a Bayesian Neural
 378 Network (BNN) with stochastic layers, where the weights follow probability distributions rather than fixed values.
 379 The uncertainty propagates through multiple stochastic forward passes, generating both attack probabilities
 380 $p(y | \mathbf{X})$ and predictive variance σ^2 . This quantifies the model confidence, distinguishing between true attacks
 381 and noise.
- 383 • **Decision & Feedback Layer :** A dynamic thresholding mechanism triggers actions based on uncertainty:
 - 384 – If $\sigma^2 >$ threshold \rightarrow Human-in-the-loop review for ambiguous cases.
 - 385 – If $\sigma^2 \leq$ threshold \rightarrow Automated mitigation.
 - 386 – Continuous model updates via Bayesian inference adapt to emerging threats, ensuring robust performance
 387 in evolving WSN environments.

389 Bayesian inference is based on Bayes' theorem, which states the following:

$$391 \quad P(H | D) = \frac{P(D | H) \cdot P(H)}{P(D)} \quad (1)$$

394 Where, $P(H | D)$ is the posterior probability of hypothesis H given data D , $P(D | H)$ is the likelihood of data D
 395 given hypothesis H , $P(H)$ is the prior probability of hypothesis H , and $P(D)$ is the marginal likelihood of data
 396 D .

397 A neural network can be represented as a function $f(x; \theta)$, where x is the input data and θ represents the
 398 weights and biases of the network. In a Bayesian Neural Network, the weights θ are treated as random variables
 399 with a prior distribution $P(\theta)$.

401 The posterior distribution of the weights given the data can be expressed as:

$$403 \quad P(\theta | D) = \frac{P(D | \theta) \cdot P(\theta)}{P(D)} \quad (2)$$

405 Where, $P(D | \theta)$ is the likelihood of the data given the weights and $P(\theta)$ is the prior distribution of the weights.
 406 For intrusion detection, the likelihood can be modeled using a softmax function for multi-class classification or
 407 a sigmoid function for binary classification.

$$410 \quad P(D | \theta) = \prod_{i=1}^N f(y_i | f(x_i; \theta)) \quad (3)$$

413 Where, y_i is the true label for input x_i . Common choices for the prior distribution $P(\theta)$ include the following
 414 cases,

- 415 – **Case 1: Gaussian prior:** $\theta \sim \mathcal{N}(0, \sigma^2)$

417 – **Case 2: Laplace prior:** $\theta \sim \text{Laplace}(0, b)$

418 Since the exact posterior $P(\theta | D)$ is often intractable, we use variational inference to approximate it. We define
419 a variational distribution $Q(\theta)$ and minimize the Kullback–Leibler (KL) divergence:
420

$$422 \quad KL(Q(\theta) \| P(\theta | D)) = \int Q(\theta) \log \frac{Q(\theta)}{P(\theta | D)} d\theta \quad (4)$$

423 The loss function for training the BNN can be derived from the evidence lower bound (ELBO) as follows:
424

$$426 \quad L = \mathbb{E}_{Q(\theta)} [\log P(D | \theta)] - KL(Q(\theta) \| P(\theta)) \quad (5)$$

427 The uncertainty in predictions can be quantified using the posterior distribution of the weights. For a new input
428 x^* , the predictive distribution is given by:
429

$$431 \quad P(y^* | x^*, D) = \int P(y^* | x^*, \theta) P(\theta | D) d\theta \quad (6)$$

432 This integral can be approximated using Monte Carlo methods or variational inference. The proposed Bayesian
433 Neural Network enhances security by quantifying uncertainty in intrusion detection, which is crucial for distinguishing
434 real attacks from noisy sensor data. It treats model weights as probability distributions rather than fixed values, enabling
435 them to capture epistemic uncertainty (model uncertainty due to limited training data) and aleatoric uncertainty
436 (inherent data noise). By integrating BNNs, WSNs gain a probabilistic defense mechanism that balances detection
437 accuracy with operational efficiency, which is critical for high-density deployments. In a traditional neural network,
438 dropout is used only during training to prevent overfitting, but in this Bayesian approach, dropout remains active
439 during both training and inference. It allows the network to generate multiple stochastic predictions for the same
440 input, effectively sampling from the posterior distribution of the model parameters. The uncertainty in predictions is
441 captured by the variability in these stochastic forward passes. Algorithm.1 shows the working of BNN algorithm to
442 detect uncertainty.
443

444 **Algorithm 1** BNN Algorithm

```
445 1: function CREATE_BNN(input_dim, output_dim)
446 2:   model ← Sequential()
447 3:   model.add(Dense(units=128, activation='relu', input_dim=input_dim))
448 4:   model.add(Dropout(rate=0.5))                                ▷ Dropout for uncertainty
449 5:   model.add(Dense(units=64, activation='relu'))
450 6:   model.add(Dropout(rate=0.5))                                ▷ Dropout for uncertainty
451 7:   model.add(Dense(units=output_dim, activation='softmax'))    ▷ Output layer
452 8:   return model
453 9: end function
454
```

455 The model is structured as a sequential neural network with dense layers and ReLU activations. The key Bayesian
456 component is the inclusion of Dropout layers with a rate of 0.5, which introduces randomness during inference. By
457 performing multiple forward passes with dropout enabled, the model produces a distribution of outputs rather than
458 a single deterministic prediction. The final layer uses a softmax activation for classification tasks, where the output
459 probabilities can be interpreted alongside their uncertainty. This approach provides a computationally efficient way to
460

469 approximate Bayesian inference without explicitly defining prior distributions over weights, as required in full Bayesian
 470 neural networks.
 471

472 2.5 Monte Carlo Dropout Sampling Process

473 The Monte Carlo (MC) Dropout sampling process enables Bayesian uncertainty estimation in deep learning models
 474 without modifying the base neural network architecture. The workflow begins by feeding preprocessed input data into
 475 a Bayesian Neural Network with active dropout layers during inference. It is a regularization technique used in neural
 476 networks to prevent overfitting. During training, dropout randomly sets a fraction of the neurons to zero. This can be
 477 mathematically represented as the following.
 478

$$480 \hat{y} = f(x; \theta * r) \quad (7)$$

481 Where, y is the output of the network with dropout, $f(x; \theta)$ is the neural network function with weights θ , and r
 482 is a binary mask vector where each element is drawn from a Bernoulli distribution $r_i \sim \text{Bernoulli}(p)$ (where p is the
 483 probability of keeping a neuron active). In a Bayesian Neural Network, we treat the weights as random variables. The
 484 dropout process can be interpreted as a way to approximate the posterior distribution of the weights. Monte Carlo
 485 sampling using dropout to estimate uncertainty in predictions. For a given input x^* , perform multiple forward passes
 486 through the network with dropout enabled. Each forward pass will yield a different output due to the random dropout
 487 mask. Let y_i^* be the output from the i -th forward pass. The outputs can be collected to form a distribution:
 488

$$489 OD = \{y_1^*, y_2^*, \dots, y_N^*\} \quad (8)$$

490 Where N is the number of Monte Carlo samples. The mean and variance of the outputs can be computed as following.
 491

492 Mean Prediction

$$493 \hat{y}^* = \frac{1}{N} \sum_{i=1}^N y_i \quad (9)$$

502 Variance (Uncertainty) Prediction

$$504 \sigma^2 = \frac{1}{N-1} \sum_{i=1}^N (y_i^* - \hat{y}^*)^2 \quad (10)$$

505 The final prediction for a given input x^* can be reported as:

- 506 • **Predicted class:** The class corresponding to the highest mean output.
- 507 • **Uncertainty:** The variance σ^2 can be used to assess the confidence in the prediction. A higher variance indicates
 508 greater uncertainty.

509 The MC Dropout retains stochasticity, executing multiple forward passes with random dropout masks applied
 510 to neurons. Each pass yields a slightly different prediction due to the model's inherent randomness, generating a
 511 distribution of output probabilities. Uncertainty is quantified by computing the variance (σ^2) across these predictions.
 512 Key variance metrics include:

- 513 • **Epistemic Uncertainty (model uncertainty):** High variance indicates insufficient training data or ambiguous
 514 inputs.

521 • **Aleatoric Uncertainty (data noise):** Captures inherent sensor measurement variability.
 522
 523 If the variance exceeds a predefined threshold, the sample is flagged as high uncertainty, triggering human review or
 524 additional verification. Conversely, low-variance predictions undergo automated mitigation. The process terminates
 525 with updated model confidence estimates, enhancing intrusion detection robustness in dynamic WSN environments. The
 526 Monte Carlo Dropout (MC Dropout) Sampling Algorithm is a practical approximation of Bayesian inference in deep
 527 neural networks, leveraging dropout layers to estimate prediction uncertainty. In this method, dropout remains active
 528 during inference (by setting `training=True`), enabling the network to produce stochastic predictions for the same input
 529 across multiple forward passes. Algorithm 2 provides the functional structure of the Monte Carlo Dropout Sampling
 530 Algorithm.
 531

Algorithm 2 Monte Carlo Dropout Sampling Algorithm

```

535 1: function MONTECARLODROPOUT(model, input_data, num_samples)
536 2:   predictions  $\leftarrow [ \ ]$ 
537 3:   for i = 1 to num_samples do
538 4:     pred  $\leftarrow$  model.predict(input_data, training = True)            $\triangleright$  Enable dropout during prediction
539 5:     append pred to predictions
540 6:   end for
541 7:   mean_prediction  $\leftarrow$  mean(predictions)
542 8:   uncertainty  $\leftarrow$  variance(predictions)                          $\triangleright$  Estimate uncertainty
543 9:   return mean_prediction, uncertainty
544 10: end function
545
  
```

546 The algorithm works by sampling predictions ‘*num_samples*’ times, each time with different neurons randomly
 547 dropped out, simulating draws from the model’s posterior distribution. The mean prediction is computed by averaging
 548 these samples, representing the final prediction, while the variance across samples quantifies the model’s uncertainty.
 549 MC Dropout is particularly useful in safety-critical applications where understanding prediction confidence is essential.
 550

551 2.6 Uncertainty-Aware Decision Workflow

552 The system starts by feeding preprocessed sensor data into the input layer as a feature vector $\mathbf{X} \in \mathbb{R}^d$. The hidden layers
 553 consist of Bayesian dense layers where weights follow probability distributions (e.g., Gaussian priors $\mathcal{N}(\mu, \sigma^2)$), enabling
 554 weight uncertainty, and Monte Carlo Dropout layers that remain active during inference, applying random masks to
 555 neurons. The output layer produces a categorical distribution over attack classes via a softmax function, where each
 556 forward pass generates slightly different predictions due to the stochastic layers. Predictive uncertainty is quantified
 557 by computing variance across multiple passes (epistemic uncertainty) and inherent noise in predictions (aleatoric
 558 uncertainty). The process ends by outputting both the attack probability distribution and an associated uncertainty
 559 measure, allowing the system to make confidence-aware security decisions.

560 Let \hat{y} be the predicted output and σ^2 be the estimated uncertainty (variance) from the model. The uncertainty can be
 561 quantified as follows:

$$U(x^*) = \sigma^2 \quad (11)$$

562 where $U(x^*)$ represents the uncertainty associated with the prediction for input x^* . Now, the threshold level can be
 563 used for decision making:
 564

- 573 • **Threshold 1: Low Uncertainty:** If $U(x^*) < \tau_1$ (where τ_1 is a predefined low uncertainty threshold), classify
574 the input as normal or as a specific type of intrusion confidently.
- 575 • **Threshold 2: Moderate Uncertainty:** If $\tau_1 \leq U(x^*) < \tau_2$ (where τ_2 is a predefined moderate uncertainty
576 threshold), flag the input for further analysis or human review.
- 577 • **Threshold 3: High Uncertainty:** If $U(x^*) \geq \tau_2$, do not make a classification and alert the system for potential
578 anomalies, indicating that the model is uncertain about the input.
- 579
- 580

581 Use feedback from the decisions made (correct or incorrect) to retrain the model periodically, enhancing its ability to
582 handle uncertainty in future predictions. Algorithm.3 provides the detailed structure of Uncertainty-Aware Decision
583 Algorithm.

Algorithm 3 Uncertainty-Aware Decision Algorithm

```

589 1: function DECISION_WORKFLOW(model, input_data)
590 2:   mean_pred, uncertainty ← MONTECARLODROPOUT(model, input_data, 100)
591 3:   if uncertainty <  $\tau_1$  then
592 4:     decision ← "Classify"                                ▷ Low uncertainty: classify confidently
593 5:   else if  $\tau_1 \leq \text{uncertainty} < \tau_2$  then
594 6:     decision ← "Review needed"                         ▷ Moderate uncertainty: flag for analysis
595 7:   else
596 8:     decision ← "Alert: Uncertain input"                ▷ High uncertainty: potential anomaly
597 9:   end if
598 10:  return decision
599 11: end function
600
601
602
603
604
605

```

606 This algorithm uses Monte Carlo Dropout to make reliable predictions while accounting for model uncertainty.
607 First, it generates multiple predictions (*num_samples*=100) and computes the mean prediction (most likely output) and
608 uncertainty (variance across samples). Based on predefined thresholds (τ_1 and τ_2), the algorithm takes different
609 actions: if uncertainty is low (below τ_1), it confidently classifies the input; if uncertainty is moderate, it flags the
610 result for human review; and if uncertainty is high (above τ_2), it raises an alert for potential anomalies. This approach
611 ensures robust decision-making in high-stakes scenarios where unreliable predictions must be detected and handled
612 appropriately.

3 Results

618 The performance of proposed Bayesian Deep Learning framework (BDLF) has compared with the existing uncertainty-
619 aware cluster-based deployment approach (UCBA) [13], Firefly algorithm (FFA) [16], enhanced intrusion detection
620 model (EIDM) [17], light-weight intelligent intrusion detection model (LIDM) [18] and Intrusion detection algorithm
621 (IDA) [29]. Here, the Network simulator (NS-2) and WSN Intrusion dataset [33] is used to execute the results. Table.2
622 provides the simulation parameters.

Table 2. Simulation Parameters

Parameters	Values
Number of sensor nodes	100
Network area	1000×1000 m
Base station location	500×500
Maximum transmission range	150 m
Packet loss probability	0.1
Attack occurrence probability	0.05
Duration of attack	10 ms
Input feature dimensions	10
Channel type	Wireless
Routing protocol	AODV
Maximum packet queue	50
Simulation time	100 s

3.1 Estimation of Accuracy

The estimation of accuracy has considered both the predictive posterior distribution and uncertainty quantification. Let us consider $f_\theta(x)$ to denote the BNN with parameters θ treated as random variables following a prior distribution $p(\theta)$. Given input data x and true label y , the predictive posterior is obtained via Bayesian marginalization:

$$p(y|x, D) = \int p(y|x, \theta) * P(\theta|D) * d\theta \quad (12)$$

where D is the training dataset and $p(\theta | D)$ is the posterior distribution over parameters. Since exact inference is intractable, By Using MC sampling with T stochastic forward passes:

$$p(y | x, D) \approx \frac{1}{T} \sum_{t=1}^T p(y | x, \theta_t) \quad \text{where } \theta_t \sim p(\theta | D) \quad (13)$$

The predicted class \hat{y} is the maximum a posteriori (MAP) estimate the following :

$$\hat{y} = \arg \max_y p(y | x, D) \quad (14)$$

The accuracy is computed as the fraction of correct predictions over N test samples:

$$A = \frac{1}{N} \sum_{i=1}^N \vartheta(\hat{y}_i = y_i) \quad (15)$$

where $\vartheta(\cdot)$ is the indicator function.

The Expected Calibration Error (ECE) is computed as follows:

$$ECE = \sum_{m=1}^M \frac{|B_m|}{N} |acc(B_m) - conf(B_m)| \quad (16)$$

where B_m denotes bins partitioning confidence scores, $acc(B_m)$ is the accuracy in bin m , and $conf(B_m)$ is the average confidence.

677 The Brier Score (BS) assesses probabilistic prediction quality and is given by:
 678

$$679 \quad 680 \quad 681 \quad BS = \frac{1}{N} \sum_{i=1}^N (p(y_i | x_i, D) - \vartheta(y_i = \hat{y}_i))^2 \quad (17)$$

682 The proposed BDL framework's accuracy is not only derived from classification performance but also validated
 683 through uncertainty calibration, ensuring robust intrusion detection in high-density WSNs under adversarial and noisy
 684 conditions. Table.3 shows the estimation of accuracy.
 685

686
 687 Table 3. Estimation of Accuracy
 688

689 690 691 692 693 694 695 696 697 698 699 700 701 702	2*Sample Size	Accuracy					
		BDLF	UCBA	FFA	EIDM	LIDM	IDA
703	100	0.951	0.852	0.823	0.824	0.785	0.756
704	200	0.955	0.854	0.803	0.823	0.782	0.752
705	300	0.961	0.858	0.806	0.826	0.784	0.754
706	400	0.965	0.862	0.809	0.829	0.786	0.756
707	500	0.971	0.866	0.812	0.832	0.788	0.758
708	600	0.975	0.872	0.815	0.835	0.795	0.766
709	700	0.981	0.874	0.818	0.838	0.792	0.762
710	800	0.985	0.878	0.821	0.841	0.794	0.764
711	900	0.991	0.882	0.824	0.844	0.796	0.766
712	1000	0.995	0.886	0.827	0.847	0.798	0.768

705 Fig.5 (a) shows the comparative analysis of accuracy. In a estimation tip, the proposed BDLF reached 99.5% accuracy.
 706 The existing UCBA reached 88.6%, FFA obtained 82.7%, EIDM reached 84.7%, LIDM obtained 79.8% and IDA reached
 707 76.8% accuracy.
 708

710 3.2 Estimation of Precision

711 The precision as the ratio of true positive prediction (TPP) to the sum of true positive prediction and false positive
 712 prediction (FPP).
 713

$$714 \quad 715 \quad P = \frac{TPP}{TPP + FPP} \quad (18)$$

716 In the Bayesian context, predictions are probabilistic, obtained via Monte Carlo (MC) sampling over T stochastic
 717 forward passes of the neural network with dropout enabled at test time. Let x denote the input data sample, and
 718 $y_i \in \{0, 1\}$ indicate whether it is an intrusion (1) or benign (0). The predictive mean for the intrusion class is the
 719 following:
 720

$$721 \quad 722 \quad 723 \quad p(y_i = 1 | x_i, D) \approx \frac{1}{T} \sum_{t=1}^T f_{\theta_t}(x_i) \quad (19)$$

724 where f_{θ_t} is the softmax output of the BNN for the intrusion class in the t -th MC sample. The final predicted label \hat{y}_i
 725 is obtained via thresholding. To compute True Positive Predictions (TPP) and False Positive Predictions (FPP), aggregate
 726 predictions over the test set D_{test} :
 727

$$729 \quad 730 \quad 731 \quad TPP = \sum_{i=1}^N \vartheta(\hat{y}_i = 1 \wedge y_i = 1) \quad \text{and} \quad FPP = \sum_{i=1}^N \vartheta(\hat{y}_i = 1 \wedge y_i = 0) \quad (20)$$

733 The Bayesian precision (P) thus becomes the following:

$$734 \quad 735 \quad P = \frac{\sum_{i=1}^N \vartheta(\hat{y}_i = 1 \wedge y_i = 1)}{\sum_{i=1}^N \vartheta(\hat{y}_i = 1 \wedge y_i = 1) + \sum_{i=1}^N \vartheta(\hat{y}_i = 1 \wedge y_i = 0)} \quad (21)$$

736 which simplifies to the standard precision expression:

$$737 \quad 738 \quad 739 \quad P = \frac{\sum_{i=1}^N \vartheta(\hat{y}_i = 1 \wedge y_i = 1)}{\sum_{i=1}^N \vartheta(\hat{y}_i = 1)} \quad (22)$$

740 To incorporate uncertainty awareness, the classification threshold may adjust based on predictive variance or entropy,
 741 reducing FP by rejecting low-confidence predictions. This ensures higher precision in security-critical WSNs, where
 742 false alarms must be minimized. The derived precision, combined with recall and uncertainty metrics, validates the
 743 framework's reliability in adversarial environments. Table.4 shows the estimation of precision.

744 Table 4. Estimation of Precision

745 2*Sample Size	Precision					
	746 BDLF	747 UCBA	748 FFA	749 EIDM	750 LIDM	751 IDA
752 100	0.931	0.832	0.783	0.843	0.765	0.736
753 200	0.935	0.834	0.783	0.803	0.762	0.732
754 300	0.941	0.838	0.786	0.806	0.764	0.734
755 400	0.945	0.842	0.789	0.809	0.766	0.736
756 500	0.951	0.846	0.792	0.812	0.768	0.738
757 600	0.955	0.852	0.795	0.815	0.774	0.746
758 700	0.961	0.854	0.798	0.818	0.772	0.742
759 800	0.965	0.858	0.801	0.821	0.774	0.744
760 900	0.971	0.862	0.804	0.824	0.776	0.746
761 1000	0.975	0.866	0.807	0.827	0.778	0.748

762 Fig.5 (b) shows the comparative analysis of precision. In a estimation tip, the proposed BDLF reached 97.5% precision.
 763 The existing UCBA reached 86.6%, FFA obtained 80.7%, EIDM reached 82.7%, LIDM obtained 77.8% and IDA reached
 764 74.8% precision.

765 3.3 Estimation of Recall

766 The recall (R) as the ratio of true positive predictions (TPP) to the sum of true positive predictions and false negative
 767 predictions (FNP).

$$768 \quad 769 \quad R = \frac{TPP}{TPP + FNP} \quad (23)$$

770 The predictions are obtained through MC sampling over T stochastic forward passes of the neural network. For
 771 a given input x_i , the predictive probability of the intrusion class ($y_i = 1$) is approximated as derived from Eq. 19. To
 772 compute TPP and FNP, predictions must be aggregated over the test set D_{test} as follows:

$$\begin{aligned} 781 \\ 782 \quad TPP &= \sum_{i=1}^N \vartheta(\hat{y}_i = 1 \wedge y_i = 1) \quad \text{and} \quad FNP = \sum_{i=1}^N \vartheta(\hat{y}_i = 0 \wedge y_i = 1) \end{aligned} \quad (24)$$

784 The Bayesian recall (R) thus becomes the following:
785

$$786 \quad R = \frac{\sum_{i=1}^N \vartheta(\hat{y}_i = 1 \wedge y_i = 1)}{\sum_{i=1}^N \vartheta(\hat{y}_i = 1 \wedge y_i = 1) + \sum_{i=1}^N \vartheta(\hat{y}_i = 0 \wedge y_i = 1)} \quad (25)$$

789 which simplifies to:
790

$$791 \quad R = \frac{\sum_{i=1}^N \vartheta(\hat{y}_i = 1 \wedge y_i = 1)}{\sum_{i=1}^N \vartheta(y_i = 1)} \quad (26)$$

794 To enhance uncertainty awareness, the threshold can be dynamically adjusted based on predictive uncertainty. For
795 instance, in high-uncertainty scenarios, the system may defer decisions or trigger additional verification, ensuring
796 robust intrusion detection while maintaining high recall. This approach is critical in high-density WSNs, where missed
797 intrusions (FNP) can compromise security. The derived recall, combined with precision and uncertainty metrics, ensures
798 the framework's effectiveness in detecting adversarial activities under uncertainty. Table.5 shows the estimation of
799 recall.
800

801
802 Table 5. Estimation of Recall
803

804 2*Sample Size	Recall					
	805 BDLF	UCBA	FFA	EIDM	LIDM	IDA
806 100	0.921	0.822	0.753	0.784	0.745	0.766
807 200	0.925	0.804	0.753	0.783	0.742	0.702
808 300	0.931	0.808	0.756	0.786	0.744	0.704
809 400	0.935	0.812	0.759	0.789	0.746	0.706
810 500	0.941	0.816	0.762	0.792	0.748	0.708
811 600	0.945	0.822	0.765	0.795	0.753	0.714
812 700	0.951	0.824	0.768	0.798	0.752	0.712
813 800	0.955	0.828	0.771	0.801	0.754	0.714
814 900	0.961	0.832	0.774	0.804	0.756	0.716
815 1000	0.965	0.836	0.777	0.807	0.758	0.718

818 Fig.5 (c) shows the comparative analysis of recall. In a estimation tip, the proposed BDLF reached 96.5% recall. The
819 existing UCBA reached 83.6%, FFA obtained 77.7%, EIDM reached 80.7%, LIDM obtained 75.8% and IDA reached 71.8%
820 recall.
821

823 3.4 Estimation of F1-Score

825 The F1-Score is the harmonic mean of precision (P) and recall (R), defined as follows:
826

$$827 \quad F1\text{-Score} = 2 \times \frac{(P \times R)}{(P + R)} \quad (27)$$

829 The precision is derived in Eq. 22 and recall is derived in Eq. 26. The predicted label \hat{y}_i is obtained by thresholding
830 the predictive probability:
831

$$\hat{y}_i = \theta(p(y_i = 1 | x_i, D) \geq \tau) \quad (28)$$

where τ is a decision threshold. The TPP, FPP, and FNP are obtained from Eq. 20 and Eq. 24. Now, the F1-Score has the following expanded form:

$$F1\text{-Score} = 2 \times \frac{\sum_{i=1}^N \theta(\hat{y}_i = 1 \wedge y_i = 1)}{\sum_{i=1}^N \theta(\hat{y}_i = 1 \wedge y_i = 1) + \sum_{i=1}^N \theta(\hat{y}_i = 1 \wedge y_i = 0) + \sum_{i=1}^N \theta(\hat{y}_i = 0 \wedge y_i = 1)} \quad (29)$$

To incorporate uncertainty awareness, the threshold τ can be adapted based on predictive uncertainty. For instance, samples with high uncertainty might be excluded from the F1-Score calculation or subjected to further scrutiny, ensuring robust performance in adversarial WSN environments. The derived F1Score, combined with uncertainty metrics, validates the framework's ability to balance precision and recall while enhancing security in high-density WSNs. Table.6 shows the estimation of F1Score.

Table 6. Estimation of F1-Score

2*Sample Size	F1-Score					
	BDLF	UCBA	FFA	EIDM	LIDM	IDA
100	0.941	0.822	0.763	0.794	0.755	0.726
200	0.945	0.824	0.763	0.793	0.752	0.722
300	0.951	0.828	0.766	0.796	0.754	0.724
400	0.955	0.832	0.769	0.799	0.756	0.726
500	0.961	0.836	0.772	0.802	0.758	0.728
600	0.965	0.842	0.775	0.805	0.765	0.736
700	0.971	0.844	0.778	0.808	0.762	0.732
800	0.975	0.848	0.781	0.811	0.764	0.734
900	0.981	0.852	0.784	0.814	0.766	0.736
1000	0.985	0.856	0.787	0.817	0.768	0.738

3.5 Estimation of Detection Rate

The detection rate (DR) is the probability that an actual intrusion is correctly identified by the system. It is expressed as the following:

$$DR = \frac{TPP}{TPP + FNP} \quad (30)$$

The TPP and FNP values are obtained from Eq. 20 and Eq. 24. Now, the estimation of DR has the following:

$$DR = \frac{\sum_{i=1}^N \theta(\hat{y}_i = 1 \wedge y_i = 1)}{\sum_{i=1}^N \theta(\hat{y}_i = 1 \wedge y_i = 1) + \sum_{i=1}^N \theta(\hat{y}_i = 0 \wedge y_i = 1)} \quad (31)$$

which simplifies to:

$$DR = \frac{\sum_{i=1}^N \theta(\hat{y}_i = 1 \wedge y_i = 1)}{\sum_{i=1}^N \theta(y_i = 1)} \quad (32)$$

In high-uncertainty scenarios, the system may lower the threshold to reduce false negatives, thereby improving the detection rate while maintaining robustness against adversarial attacks. This approach is particularly critical in

high-density WSNs, where missed intrusions can have severe security implications. The derived DR, combined with precision and uncertainty metrics, ensures the framework's effectiveness in identifying intrusions under uncertain and adversarial conditions.

The Bayesian framework allows for the computation of uncertainty-aware detection rate DR_μ by considering only predictions with low uncertainty as shown in the following:

$$DR_\mu = \frac{\sum_{i=1}^N \vartheta(\hat{y}_i = 1 \wedge y_i = 1 \wedge \mu(x_i) \leq \epsilon)}{\sum_{i=1}^N \vartheta(y_i = 1)} \quad (33)$$

Where, $H(x_i)$ is the entropy of the predictive distribution for sample x_i . This refinement ensures that the reported DR reflects confident and reliable detections, further enhancing the security of the WSN. The integration of uncertainty quantification into the DR metric underscores the framework's capability to provide trustworthy intrusion detection in dynamic and resource-constrained environments.

Table.7 shows the estimation of estimation of detection rate.

Table 7. Estimation of Detection Rate

2*Sample Size	Detection Rate					
	BDLF	UCBA	FFA	EIDM	LIDM	IDA
100	0.911	0.792	0.743	0.774	0.735	0.766
200	0.915	0.794	0.743	0.773	0.732	0.702
300	0.921	0.798	0.746	0.776	0.734	0.704
400	0.925	0.802	0.749	0.779	0.736	0.706
500	0.931	0.806	0.752	0.782	0.738	0.708
600	0.935	0.812	0.755	0.785	0.743	0.713
700	0.941	0.814	0.758	0.788	0.742	0.712
800	0.945	0.818	0.761	0.791	0.744	0.714
900	0.951	0.822	0.764	0.794	0.746	0.716
1000	0.955	0.826	0.767	0.797	0.748	0.718

Fig.5 (e) shows the comparative analysis of detection rate. In a estimation tip, the proposed BDLF reached 95.5% detection rate. The existing UCBA reached 82.6%, FFA obtained 76.7%, EIDM reached 79.7%, LIDM obtained 74.8% and IDA reached 71.8% detection rate.

3.6 Estimation of False Alarm Rate

The false alarm rate (FAR) as the probability that a benign instance is incorrectly classified as an intrusion. It is expressed as the following,

$$FAR = \frac{FPP}{FPP + TNP} \quad (34)$$

The FPP and TNP values are obtained from Eq. 20 and Eq. 24. Now, the estimation of FAR has the following form:

$$FAR = \frac{\sum_{i=1}^N \vartheta(\hat{y}_i = 1 \wedge y_i = 0)}{\sum_{i=1}^N \vartheta(\hat{y}_i = 1 \wedge y_i = 0) + \sum_{i=1}^N \vartheta(\hat{y}_i = 0 \wedge y_i = 0)} \quad (35)$$

which simplifies to:

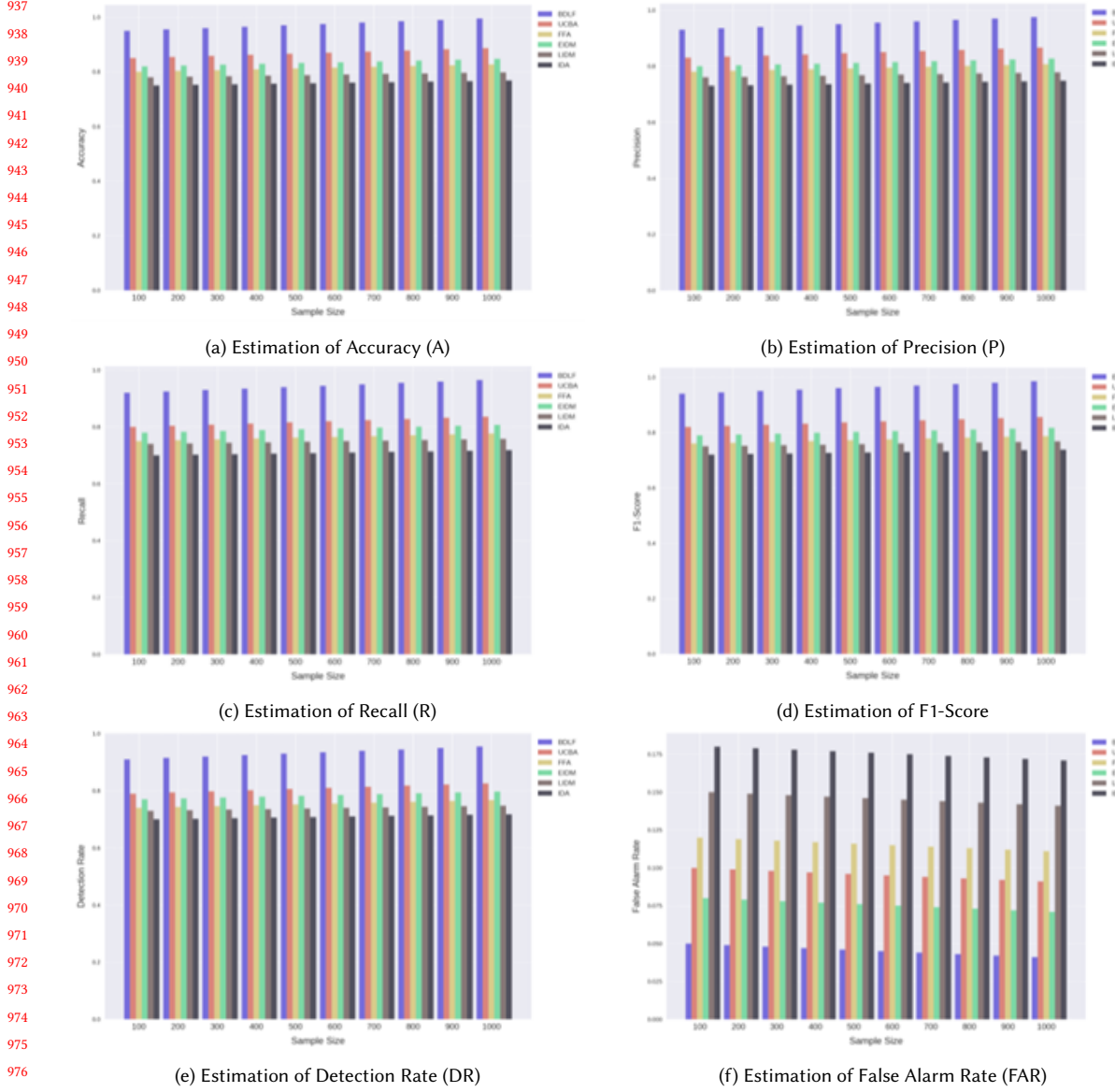


Fig. 5. Comparative analysis of performance metrics across different sample sizes for intrusion detection models.

$$FAR = \frac{\sum_{i=1}^N \vartheta(\hat{y}_i = 1 \wedge y_i = 0)}{\sum_{i=1}^N \vartheta(y_i = 0)} \quad (36)$$

In high-uncertainty scenarios, the system may increase the threshold to reduce false positives, thereby lowering the FAR while maintaining detection accuracy. This adjustment is critical in high-density WSNs, where false alarms can lead to unnecessary resource consumption and undermine trust in the intrusion detection system.

The Bayesian framework also enables the computation of uncertainty-aware FAR (FAR_u) by considering only predictions with low uncertainty:

$$FAR_U = \frac{\sum_{i=1}^N \vartheta(\hat{y}_i = 1 \wedge y_i = 0 \wedge \mu(x_i) \leq \epsilon)}{\sum_{i=1}^N \vartheta(y_i = 0)} \quad (37)$$

This refinement ensures that the reported FAR reflects confident and reliable classifications, further enhancing the security and efficiency of the WSN. The integration of uncertainty quantification into the FAR metric underscores the framework's capability to minimize false alarms while maintaining robust intrusion detection in dynamic and adversarial environments. Table.8 shows the estimation of false alarm rate.

Table 8. Estimation of False Alarm Rate

2*Sample Size	False Alarm Rate					
	BDLF	UCBA	FFA	EIDM	LIDM	IDA
100	0.051	0.122	0.123	0.084	0.155	0.186
200	0.049	0.099	0.119	0.079	0.149	0.179
300	0.047	0.101	0.121	0.081	0.151	0.181
400	0.045	0.103	0.123	0.083	0.153	0.183
500	0.043	0.105	0.125	0.085	0.155	0.185
600	0.041	0.107	0.127	0.087	0.157	0.187
700	0.039	0.109	0.129	0.089	0.159	0.189
800	0.037	0.111	0.131	0.091	0.161	0.191
900	0.035	0.113	0.133	0.093	0.163	0.193
1000	0.041	0.091	0.111	0.071	0.141	0.171

Fig.5 (f) shows the comparative analysis of false alarm rate. In a estimation tip, the proposed BDLF reached 4.1% false alarm. The existing UCBA reached 9.1%, FFA obtained 11.1%, EIDM reached 7.1%, LIDM obtained 14.1% and IDA reached 17.1% false alarm.

4 Discussion

The predictive entropy (PE) quantifies the uncertainty in the model's predictions by measuring the information content of the predictive posterior distribution. For a test sample x_t , the PE is derived from the MC-sampled class probabilities has the following,

$$p(y_i = k | x_i, D) \approx \frac{1}{T} \sum_{t=1}^T f_{\theta_t}(x_i)_k \quad (38)$$

$$PE(x_i) = - \sum_{k=1}^K p(y_i = k | x_i, D) \log p(y_i = k | x_i, D) \quad (39)$$

where K is the number of classes. High predictive entropy (PE) indicates ambiguous or uncertain predictions, which is critical for flagging suspicious activities in WSNs.

The Brier Score (BS) evaluates the accuracy of probabilistic predictions by measuring the mean squared error between predicted probabilities and true labels. For binary intrusion detection ($K = 2$):

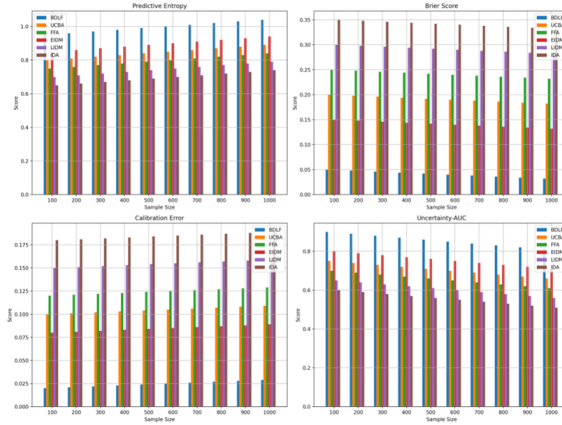


Fig. 6. Performance analysis

$$BS = \frac{1}{N} \sum_{i=1}^N (p(y_i = 1 | x_i, D) - \vartheta(y_i = 1))^2 \quad (40)$$

where $\vartheta(\cdot)$ is the indicator function. A lower BS indicates better-calibrated predictions, which is essential for reliable threat assessment.

ECE assesses how well the model's confidence aligns with its accuracy. Predictions are binned into M intervals B_m based on confidence scores (e.g., $p(y_i = 1 | x_i, D)$). ECE is computed as:

$$ECE = \sum_{m=1}^M \frac{|B_m|}{N} |acc(B_m) - conf(B_m)| \quad (41)$$

Where, $acc(B_m)$ and $conf(B_m)$ are the accuracy and average confidence in bin B_m , respectively. Low ECE ensures that high-confidence predictions are trustworthy, which is vital for security decisions.

Uncertainty AUC (UAUC) evaluates the model's ability to rank uncertain samples higher than certain ones. Let $H(x_i)$ be the entropy of x_i , and $E_i \in \{0, 1\}$ indicate whether the prediction was incorrect (1) or correct (0). The UAUC is the area under the ROC curve plotting the true positive rate (uncertainty for errors) against the false positive rate (uncertainty for correct predictions) across varying entropy thresholds.

$$UAUC = \int_0^1 TPR(h) \cdot FPR(h) dh \quad (42)$$

Where,

$$TPR(h) = P(H(x_i) \geq h | E_i = 1)$$

$$FPR(h) = P(H(x_i) \geq h | E_i = 0)$$

A $UAUC > 0.5$ indicates that the model effectively uses uncertainty to flag errors. Table 9 shows the estimation of predictive entropy.

Fig.6 (a) shows the performance analysis of predictive entropy. In a estimation tip, the proposed BDLF reached 1.04 predictive entropy. The existing UCBA reached 0.89, FFA obtained 0.84, EIDM reached 0.94, LIDM obtained 0.79 and IDA reached 0.74 predictive entropy. Table.10 shows the estimation of brier score.

Table 9. Estimation of Predictive Entropy

2*Sample Size	Predictive Entropy					
	BDLF	UCBA	FFA	EIDM	LIDM	IDA
100	0.95	0.80	0.75	0.85	0.70	0.65
200	0.96	0.81	0.76	0.86	0.71	0.66
300	0.97	0.82	0.77	0.87	0.72	0.67
400	0.98	0.83	0.78	0.88	0.73	0.68
500	0.99	0.84	0.79	0.89	0.74	0.69
600	1.00	0.85	0.80	0.90	0.75	0.70
700	1.01	0.86	0.81	0.91	0.76	0.71
800	1.02	0.87	0.82	0.92	0.77	0.72
900	1.03	0.88	0.83	0.93	0.78	0.73
1000	1.04	0.89	0.84	0.94	0.79	0.74

Table 10. Estimation of Brier Score

Sample Size	BDLF	UCBA	FFA	EIDM	LIDM	IDA
100	0.050	0.200	0.250	0.150	0.300	0.350
200	0.048	0.198	0.248	0.148	0.298	0.348
300	0.046	0.196	0.246	0.146	0.296	0.346
400	0.044	0.194	0.244	0.144	0.294	0.344
500	0.042	0.192	0.242	0.142	0.292	0.342
600	0.040	0.190	0.240	0.140	0.290	0.340
700	0.038	0.188	0.238	0.138	0.288	0.338
800	0.036	0.186	0.236	0.136	0.286	0.336
900	0.034	0.184	0.234	0.134	0.284	0.334
1000	0.032	0.182	0.232	0.132	0.282	0.332

Fig.6 (b) shows the performance analysis of brier score. In a estimation tip, the proposed BDLF reached 0.032 brier score. The existing UCBA reached 0.182, FFA obtained 0.232, EIDM reached 0.132, LIDM obtained 0.282 and IDA reached 0.332 brier score. Table.11 shows the estimation of estimated calibration error.

Table 11. Estimation of Estimated Calibration Error

Sample Size	BDLF	UCBA	FFA	EIDM	LIDM	IDA
100	0.02	0.10	0.12	0.08	0.15	0.18
200	0.021	0.101	0.121	0.081	0.151	0.181
300	0.022	0.102	0.122	0.082	0.152	0.182
400	0.023	0.103	0.123	0.083	0.153	0.183
500	0.024	0.104	0.124	0.084	0.154	0.184
600	0.025	0.105	0.125	0.085	0.155	0.185
700	0.026	0.106	0.126	0.086	0.156	0.186
800	0.027	0.107	0.127	0.087	0.157	0.187
900	0.028	0.108	0.128	0.088	0.158	0.188
1000	0.029	0.109	0.129	0.089	0.159	0.189

1145 Fig.6 (c) shows the performance analysis of estimated calibration error. In a estimation tip, the proposed BDLF
1146 reached 0.029 estimated calibration error. The existing UCBA reached 0.109, FFA obtained 0.129, EIDM reached 0.089,
1147 LIDM obtained 0.159 and IDA reached 0.189 estimated calibration error. Table.12 shows the estimation of Uncertainty
1148 AUC.
1149

1150 Table 12. Estimation of Uncertainty AUC
1151

Sample Size	BDLF	UCBA	FFA	EIDM	LIDM	IDA
100	0.90	0.75	0.70	0.80	0.65	0.60
200	0.89	0.74	0.69	0.79	0.64	0.59
300	0.88	0.73	0.68	0.78	0.63	0.58
400	0.87	0.72	0.67	0.77	0.62	0.57
500	0.86	0.71	0.66	0.76	0.61	0.56
600	0.85	0.70	0.65	0.75	0.60	0.55
700	0.84	0.69	0.64	0.74	0.59	0.54
800	0.83	0.68	0.63	0.73	0.58	0.53
900	0.82	0.67	0.62	0.72	0.57	0.52
1000	0.81	0.66	0.61	0.71	0.56	0.51

1164
1165 Fig.6 (d) shows the performance analysis of Uncertainty AUC. In a estimation tip, the proposed BDLF reached 0.81
1166 Uncertainty AUC. The existing UCBA reached 0.66, FFA obtained 0.61, EIDM reached 0.71, LIDM obtained 0.56 and IDA
1167 reached 0.51 Uncertainty AUC.
1168

1169 5 Conclusion

1170 The proposed Bayesian Deep Learning framework provides a robust, probabilistic approach to enhancing security
1171 by quantifying and leveraging predictive uncertainty. The BDL framework employs Monte Carlo (MC) dropout and
1172 Bayesian neural networks to generate stochastic forward passes, enabling the estimation of predictive entropy, variance,
1173 and confidence intervals alongside intrusion classifications. This allows the system to distinguish between certain
1174 and uncertain predictions, flagging ambiguous samples for further analysis—critical in adversarial and noisy WSN
1175 environments where false positives and negatives can degrade security. The model achieved 99.5% accuracy, 97.5%
1176 precision, 96.5% recall, 98.5% f1-score, 95.5% detection rate and 4.1% false alarm rate. The framework outperforms
1177 deterministic deep learning models in detecting novel and adversarial attacks while maintaining computational efficiency.
1178 Future work may explore distributed Bayesian inference for scalability in ultra-dense WSNs and adversarial training to
1179 further harden the model against evasion attacks. Ultimately, this approach establishes a trustworthy, adaptive, and
1180 resilient intrusion detection system crucial for securing next-generation IoT and industrial WSN deployments.
1181

1182 Declarations

1183 Funding

1184 This research did not receive any specific grant from funding agencies in the public, commercial, or not-for-profit sectors.
1185

1186 Conflicts of interest

1187 The authors declare that they have no known competing financial interests or personal relationships that could have
1188 appeared to influence the work reported in this paper.
1189

Ethical approval

This article does not contain any studies with human participants or animals performed by any of the authors.

Authors' contributions

Author 1: Conceptualization, methodology, model implementation, experiments, and writing – original draft.

Author 2: Supervision, validation, critical review, and editing.

References

- [1] W. Liang, Y. Li, J. Xu, Z. Qin, D. Zhang, and K. C. Li, "QoS prediction and adversarial attack protection for distributed services under DlaaS," *IEEE Transactions on Computers*, vol. 73, no. 3, pp. 669–682, 2023.
- [2] M. Gazzan and F. T. Sheldon, "Novel ransomware detection exploiting uncertainty and calibration quality measures using deep learning," *Information*, vol. 15, no. 5, p. 262, 2024.
- [3] S. Y. Kuo, Y. H. Chou, and C. Y. Chen, "Quantum-inspired algorithm for cyber-physical visual surveillance deployment systems," *Computer Networks*, vol. 117, pp. 5–18, 2017.
- [4] Z. Fei, B. Li, S. Yang, C. Xing, H. Chen, and L. Hanzo, "A survey of multi-objective optimization in wireless sensor networks: Metrics, algorithms, and open problems," *IEEE Communications Surveys & Tutorials*, vol. 19, no. 1, pp. 550–586, 2016.
- [5] S. Ismail, K. Shah, H. Reza, R. Marsh, and E. Grant, "Toward management of uncertainty in self-adaptive software systems: IoT case study," *Computers*, vol. 10, no. 3, p. 27, 2021.
- [6] V. P. Illiano, A. Paudice, L. Munoz-González, and E. C. Lupu, "Determining resilience gains from anomaly detection for event integrity in wireless sensor networks," *ACM Transactions on Sensor Networks (TOSN)*, vol. 14, no. 1, pp. 1–35, 2018.
- [7] A. P. Vedurmudi, K. Milicevic, G. Kok, B. X. Yong, L. Xu, G. Zheng, *et al.*, "Automation in sensor network metrology: An overview of methods and their implementations," *Measurement: Sensors*, p. 101799, 2025.
- [8] S. Ahamad and R. Gupta, "Uncertainty modelling in performability prediction for safety-critical systems," *Arabian Journal for Science and Engineering*, pp. 1–15, 2024.
- [9] C. Nakas, D. Kandris, and G. Visvardis, "Energy efficient routing in wireless sensor networks: A comprehensive survey," *Algorithms*, vol. 13, no. 3, p. 72, 2020.
- [10] A. A. Mehta, A. A. Padaria, D. J. Bavisi, V. Ukani, P. Thakkar, R. Geddam, *et al.*, "Securing the future: A comprehensive review of security challenges and solutions in advanced driver assistance systems," *IEEE Access*, vol. 12, pp. 643–678, 2023.
- [11] M. Wei, C. Rong, E. Liang, and Y. Zhuang, "An intrusion detection mechanism for IPv6-based wireless sensor networks," *International Journal of Distributed Sensor Networks*, vol. 18, no. 3, p. 15501329221077922, 2022.
- [12] G. G. Gebremariam, J. Panda, and S. J. C. S. Indu, "Design of advanced intrusion detection systems based on hybrid machine learning techniques in hierarchically wireless sensor networks," *Connection Science*, vol. 35, no. 1, p. 2246703, 2023.
- [13] M. R. Senouci and A. Mellouk, "A robust uncertainty-aware cluster-based deployment approach for WSNs: Coverage, connectivity, and lifespan," *Journal of Network and Computer Applications*, vol. 146, p. 102414, 2019.
- [14] J. Talpini, F. Sartori, and M. Savi, "Enhancing trustworthiness in ML-based network intrusion detection with uncertainty quantification," *Journal of Reliable Intelligent Environments*, vol. 10, no. 4, pp. 501–520, 2024.
- [15] R. Garg, T. Gulati, and S. Kumar, "Wormhole attack detection and recovery for secure range free localization in large-scale wireless sensor networks," *Peer-to-Peer Networking and Applications*, vol. 16, no. 6, pp. 2833–2849, 2023.
- [16] M. Karthikeyan, D. Manimegalai, and K. RajaGopal, "Firefly algorithm based WSN-IoT security enhancement with machine learning for intrusion detection," *Scientific Reports*, vol. 14, no. 1, p. 231, 2024.
- [17] G. Liu, H. Zhao, F. Fan, G. Liu, Q. Xu, and S. Nazir, "An enhanced intrusion detection model based on improved kNN in WSNs," *Sensors*, vol. 22, no. 4, p. 1407, 2022.
- [18] J. S. Pan, F. Fan, S. C. Chu, H. Q. Zhao, and G. Y. Liu, "A lightweight intelligent intrusion detection model for wireless sensor networks," *Security and Communication Networks*, vol. 2021, no. 1, p. 5540895, 2021.
- [19] K. Ramana, A. Revathi, A. Gayathri, R. H. Jhaveri, C. L. Narayana, and B. N. Kumar, "WOGRU-IDS—An intelligent intrusion detection system for IoT assisted wireless sensor networks," *Computer Communications*, vol. 196, pp. 195–206, 2022.
- [20] H. Sadia, S. Farhan, Y. U. Haq, R. Sana, T. Mahmood, S. A. O. Bahaj, and A. R. Khan, "Intrusion detection system for wireless sensor networks: A machine learning based approach," *IEEE Access*, vol. 12, pp. 52565–52582, 2024.
- [21] M. S. Alsahl, M. M. Almasri, M. Al-Akhras, A. I. Al-Issa, and M. Alawairdh, "Evaluation of machine learning algorithms for intrusion detection system in WSN," *International Journal of Advanced Computer Science and Applications*, vol. 12, no. 5, 2021.
- [22] Z. Jingjing, Y. Tongyu, Z. Jilin, Z. Guohao, L. Xuefeng, and P. Xiang, "Intrusion detection model for wireless sensor networks based on MC-GRU," *Wireless Communications and Mobile Computing*, vol. 2022, no. 1, p. 2448010, 2022.

- 1249 [23] A. Arkan and M. Ahmadi, "An unsupervised and hierarchical intrusion detection system for software-defined wireless sensor networks," *The Journal*
1250 *of Supercomputing*, vol. 79, no. 11, pp. 11844–11870, 2023.
- 1251 [24] M. A. Talukder, S. Sharmin, M. A. Uddin, M. M. Islam, and S. Aryal, "MLSTL-WSN: Machine learning-based intrusion detection using SMOTETomek
1252 in WSNs," *International Journal of Information Security*, vol. 23, no. 3, pp. 2139–2158, 2024.
- 1253 [25] H. M. Saleh, H. Marouane, and A. Fakhfakh, "Stochastic gradient descent intrusions detection for wireless sensor network attack detection system
1254 using machine learning," *IEEE Access*, vol. 12, pp. 3825–3836, 2024.
- 1255 [26] O. Ahmed, "Enhancing intrusion detection in wireless sensor networks through machine learning techniques and context awareness integration,"
1256 *International Journal of Mathematics, Statistics, and Computer Science*, vol. 2, pp. 244–258, 2024.
- 1257 [27] S. Subramani and M. Selvi, "Multi-objective PSO based feature selection for intrusion detection in IoT based wireless sensor networks," *Optik*,
1258 vol. 273, p. 170419, 2023.
- 1259 [28] M. Safaldin, M. Otair, and L. Abualigah, "Improved binary gray wolf optimizer and SVM for intrusion detection system in wireless sensor networks,"
1260 *Journal of Ambient Intelligence and Humanized Computing*, vol. 12, pp. 1559–1576, 2021.
- 1261 [29] J. Jin, "Intrusion detection algorithm and simulation of wireless sensor network under Internet environment," *Journal of Sensors*, vol. 2021, no. 1,
1262 p. 9089370, 2021.
- 1263 [30] K. Madhuri, "A new level intrusion detection system for node level drop attacks in wireless sensor network," *Journal of Algebraic Statistics*, vol. 13,
1264 no. 1, pp. 159–168, 2022.
- 1265 [31] M. Otair, O. T. Ibrahim, L. Abualigah, M. Altalhi, and P. Sumari, "An enhanced grey wolf optimizer-based particle swarm optimizer for intrusion
1266 detection system in wireless sensor networks," *Wireless Networks*, vol. 28, no. 2, pp. 721–744, 2022.
- 1267 [32] K. Hussain, Y. Xia, A. N. Omaizah, T. Manzoor, and K. Jalil, "Hybrid of WOA-ABC and proposed CNN for intrusion detection system in wireless
1268 sensor networks," *Optik*, vol. 271, p. 170145, 2022.
- 1269
1270
1271
1272
1273
1274
1275
1276
1277
1278
1279
1280
1281
1282
1283
1284
1285
1286
1287
1288
1289
1290
1291
1292
1293
1294
1295
1296
1297
1298
1299
1300